

Supplementary information for

**Structural basis of the mechanisms of action and immunity of  
lactococcin A, a class II<sub>d</sub> bacteriocin**

Ruilian Li<sup>1,#</sup>, Jinsong Duan<sup>1,#</sup>, Yicheng Zhou<sup>1,2</sup>, Jiawei Wang<sup>1,\*</sup>

<sup>1</sup>State Key Laboratory of Membrane Biology, Beijing Frontier Research Center for  
Biological Structure, School of Life Sciences, Tsinghua University, Beijing 100084, P. R.

China

<sup>2</sup>1511 E Florida Ave Apt 102B, Urbana Illinois, 61802 USA

\*Correspondence to [jwwang@tsinghua.edu.cn](mailto:jwwang@tsinghua.edu.cn)

This file includes:

- Figures S1-S5 (incl. figure legends)
- SI References

## Supplementary Figures

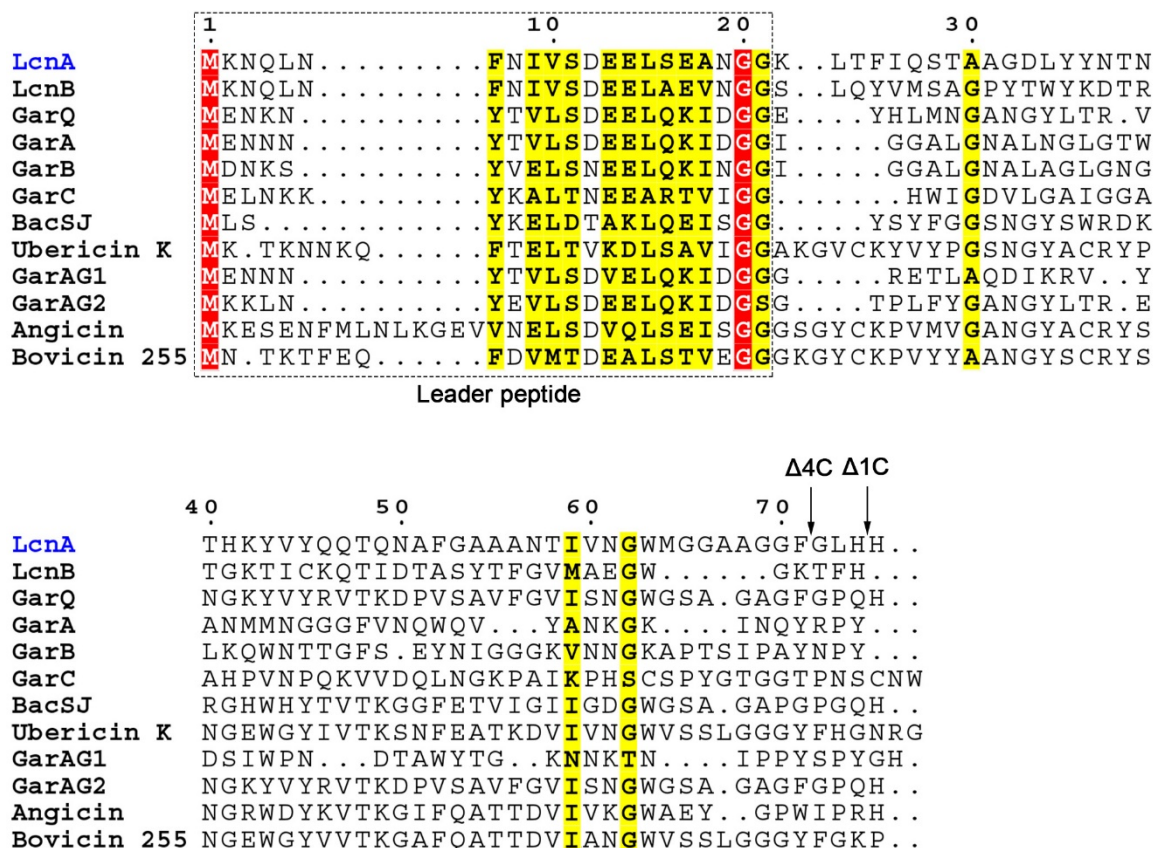


**Fig. S1. Sequence alignment of class IId bacteriocin precursor peptides commonly utilizing the mannose phosphotransferase system (man-PTS) as the receptor.**

Maturation of the bacteriocins occurs by cleavage of the leader peptides (highlighted in dashed box) after the GG/GS motif, which is coupled to the exportation of the mature peptide out of the cell by an ABC transporter. Sequences were aligned with the program ClustalW (1). The listed bacteriocins include LcnA (lactococcin A), LcnB (lactococcin B), GarQ (Garvicin Q), GarA (Garvicin A), GarB (Garvicin B), GarC (Garvicin C), BacSJ, Ubericin K, GarAG1 (Garvicin AG1), GarAG2 (Garvicin

AG2), Angicin, Bovicin 255. The C-terminal truncation positions of LcnA variants ( $\Delta 1C$  and  $\Delta 4C$ ) in Fig. 4F are indicated with the arrows.

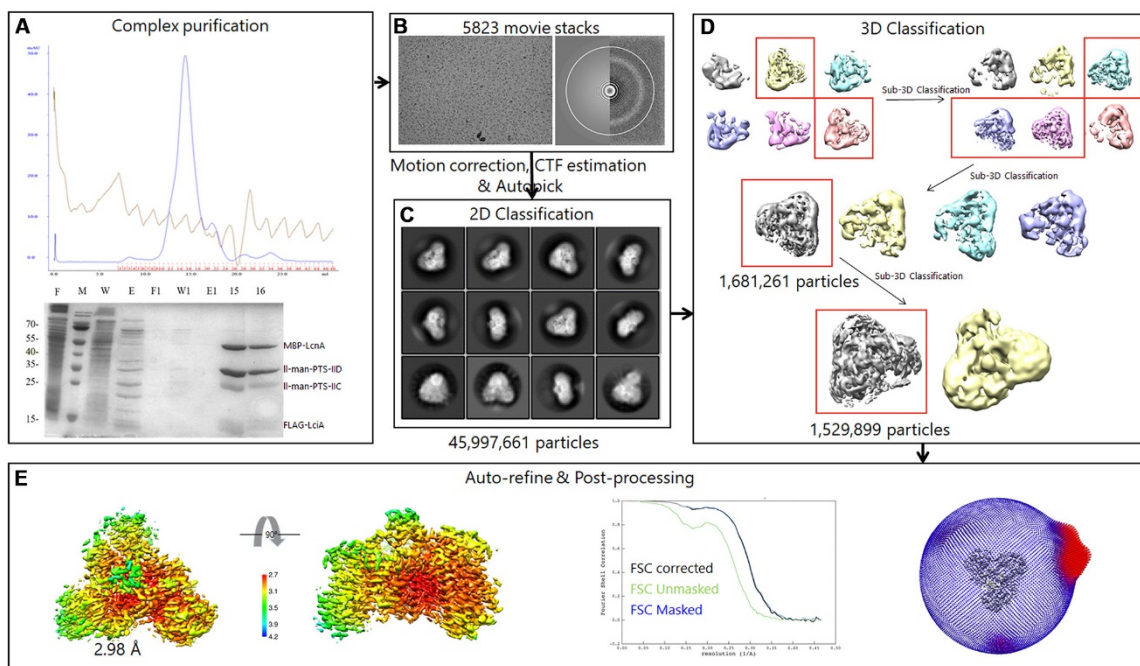


**Fig. S2. Flowchart of the structural determination of the bacteriocin-immunity complex of *L. lactis***

- (A) Purification of the complex. A representative size exclusion chromatogram of the complex is shown. The indicated peak fractions were resolved on SDS-PAGE and visualized by Coomassie blue staining.
- (B) A representative cryo-electron microscopy (cryo-EM) micrograph and power spectra. White circles indicate the estimated resolution limits of micrographs.
- (C) Representative cryo-EM 2D class averages of the complex.
- (D) 3D classification to remove ill-conditioned particles.
- (E) Auto-refine and post-processing steps. From left to right: Local-resolution map for the 3D cryo-EM reconstruction map (2). The gold-standard Fourier shell correlation (FSC) curves for the 3D reconstruction (3). Direction distribution of the particles of the final reconstruction map.



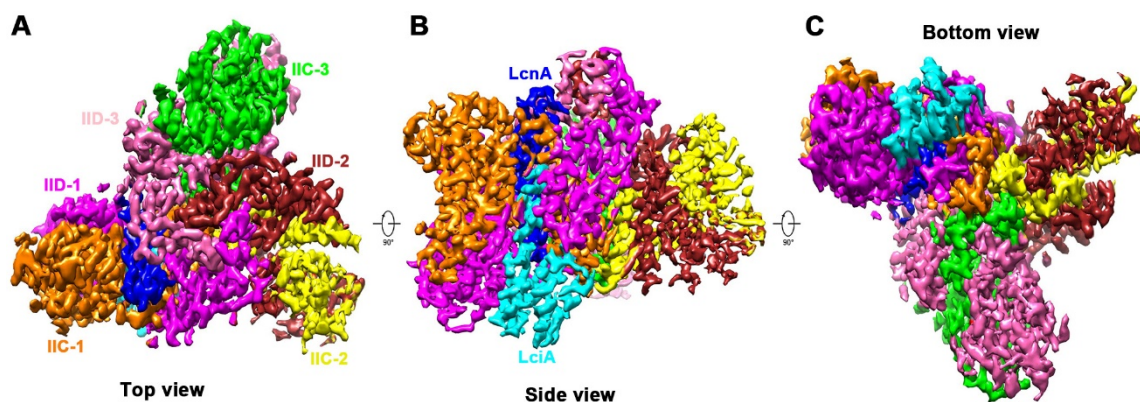


**Fig. S3. Cryo-EM map of the bacteriocin–receptor–immunity complex of *L. lactis***

(A) Viewed from the extracellular side of the membrane, as shown in Fig. 1A. The bacteriocin (blue), immunity protein (cyan), and ManY/IIC (orange, yellow, green) and ManZ/IID (magenta, brown, pink) components of the man-PTS are colored differently.

(B) Viewed within the plane of the membrane, as shown in Fig. 1B.

(C) Viewed from the cytosolic side of the membrane.

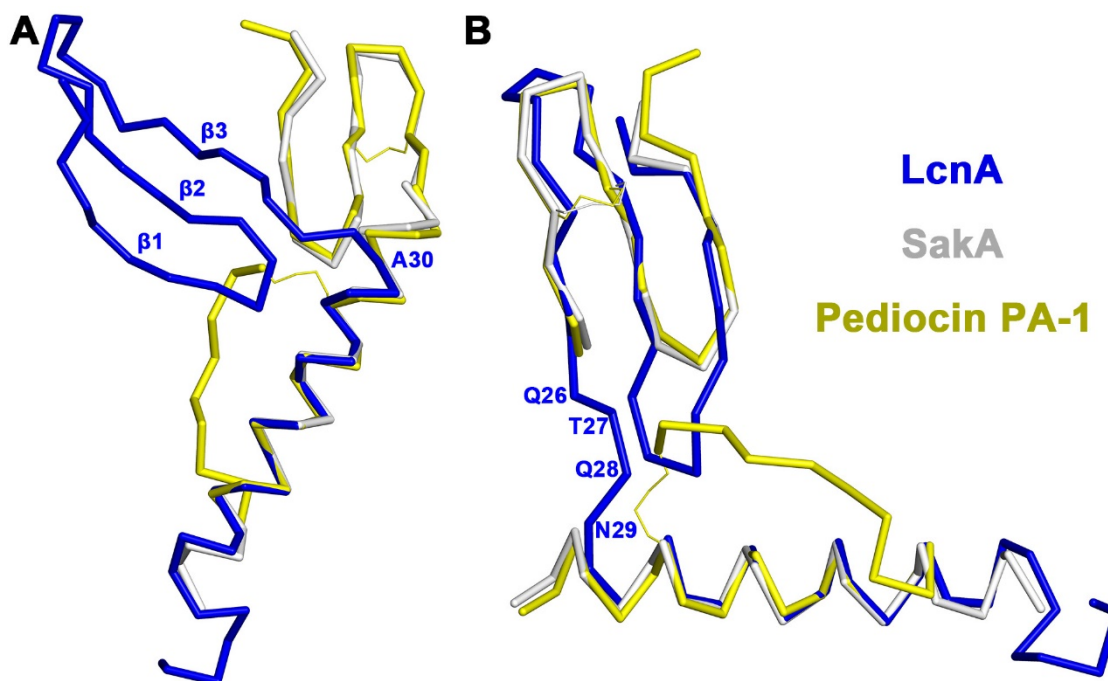
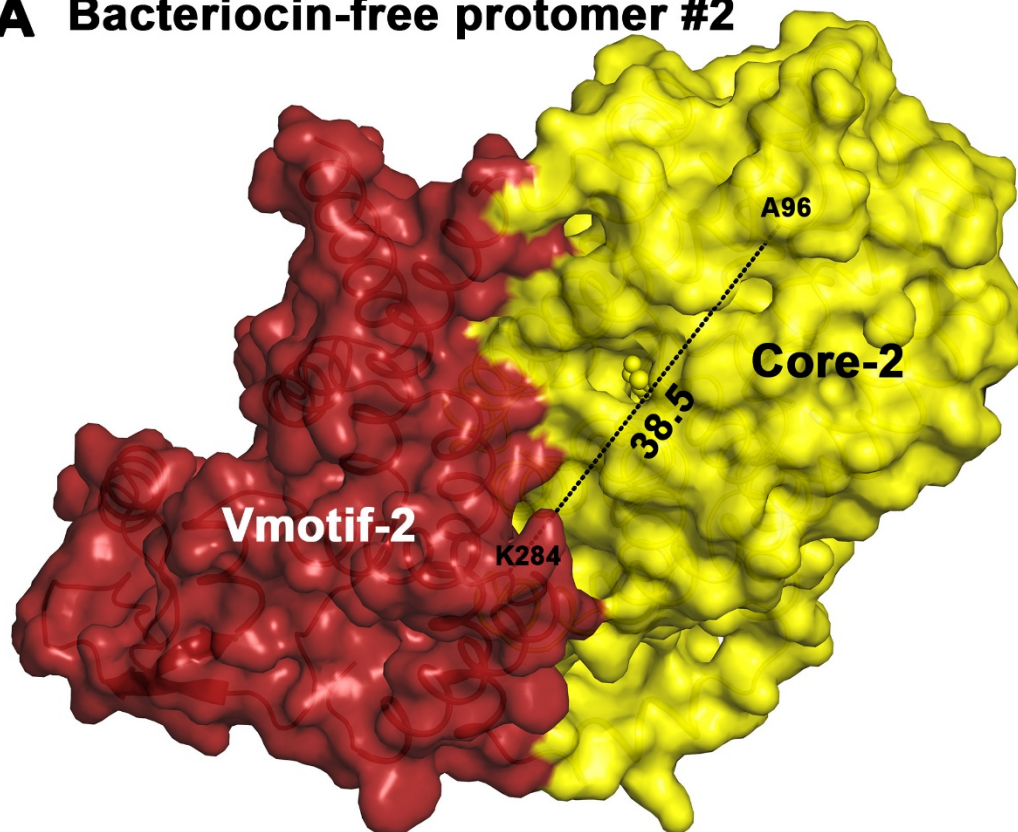


**Fig. S4. Structural alignment of class IIb bacteriocin LcnA as well as class IIa bacteriocins SakA, pediocin PA-1**

- (A) The C-terminal helical parts of three bacteriocins were aligned. LcnA is colored in blue, SakA in white, and pediocin PA-1 in yellow.
- (B) The N- and C-terminal parts of three bacteriocins were aligned separately. The disulfide bonds in SakA and pediocin PA-1 are shown as stick representations.

**A Bacteriocin-free protomer #2**



**B Bacteriocin-free protomer #3**

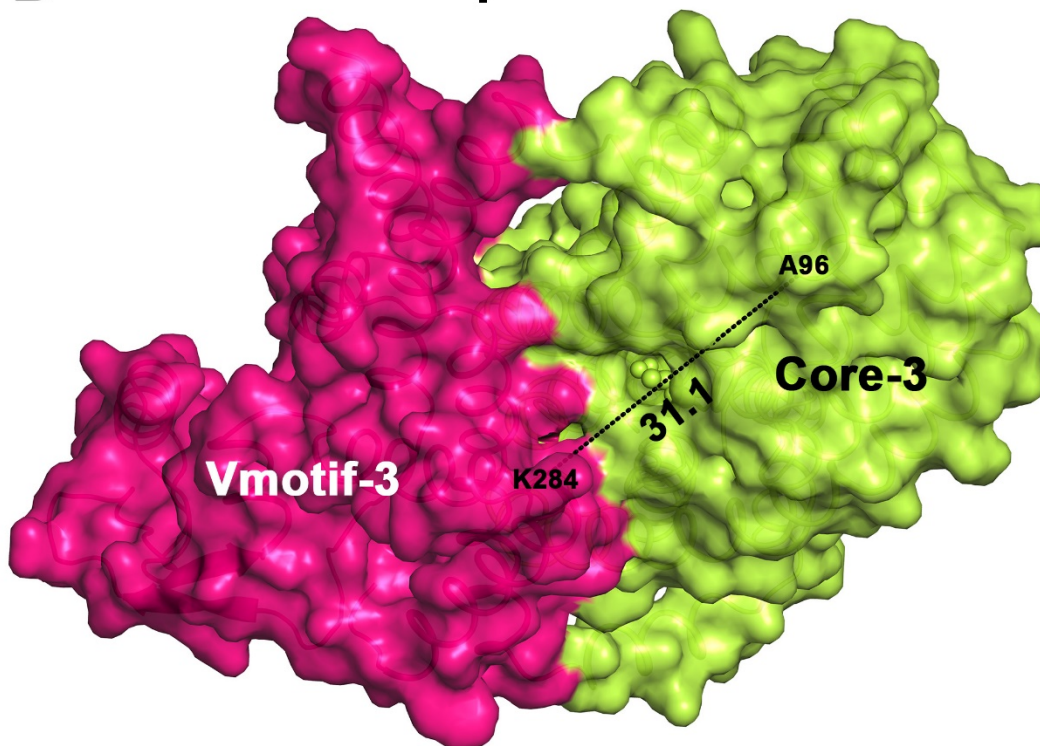




**Fig. S5. Relationship between the Vmotif and Core domains of the bacteriocin-free man-PTS in protomers #2 and #3 of the complex.**

- (A) In protomer #2, the distance between residues A96 and K284 is 38.5 Å.
- (B) In protomer #3, the corresponding distance reduces to 31.1 Å as a result of the minor rotation of the Core-3 domain towards the membrane relative to the Vmotif domain.

## References

1. Thompson JD, Gibson TJ, Higgins DG. 2002. Multiple sequence alignment using ClustalW and ClustalX. *Curr Protoc Bioinformatics* Chapter 2:Unit 2.3.
2. Kucukelbir A, Sigworth FJ, Tagare HD. 2014. Quantifying the local resolution of cryo-EM density maps. *Nat Methods* 11:63-5.
3. Rosenthal PB, Henderson R. 2003. Optimal determination of particle orientation, absolute hand, and contrast loss in single-particle electron cryomicroscopy. *J Mol Biol* 333:721-45.